Can Aerosols Be Trapped in Open Flows?

Rafael D. Vilela[1] and Adilson E. Motter[2]

[1]*Max Planck Institute for the Physics of Complex Systems, 01187 Dresden, Germany*

[2]*Department of Physics and Astronomy, Northwestern University, Evanston, Illinois 60208, USA*

(Received 21 November 2006; revised manuscript received 10 June 2007; published 28 December 2007)

The fate of aerosols in open flows is relevant in a variety of physical contexts. Previous results are consistent with the assumption that such finite-size particles always escape in open chaotic advection. Here we show that a different behavior is possible. We analyze the dynamics of aerosols both in the absence and presence of gravitational effects, and both when the dynamics of the fluid particles is hyperbolic and nonhyperbolic. Permanent trapping of aerosols much heavier than the advecting fluid is shown to occur in all these cases. This phenomenon is determined by the occurrence of multiple vortices in the flow and is predicted to happen for realistic particle-fluid density ratios.

DOI: 10.1103/PhysRevLett.99.264101 PACS numbers: 05.45.−a, 47.52.+j, 47.55.Kf

In open chaotic advection [1], fluid particles are injected into some domain containing a chaotic saddle [2], where they move chaotically for a finite amount of time until they finally escape. This is the history of almost all the injected particles in the typical case where the fluid is incompressible. When instead *finite-size* particles are injected into the domain, the outcome can be fundamentally different [3]. The reason is that these particles are subjected to new forces, in particular, the Stokes drag. Their dynamics is dissipative, allowing the existence of attractors where the particles can be trapped. This has been shown to be typical in the case of *bubbles*, i.e., finite-size particles less dense than the fluid [4]. On the other hand, previous studies on specific open flows support the assumption that finite-size particles denser than the fluid, called *aerosols*, always escape [4,5]. Moreover, there is evidence that aerosols escape even faster than the particles of fluid [4]. The physical reason for this is that chaotic saddles are usually associated with the occurrence of vortices. Bubbles in vortices tend to move inward, therefore possibly being trapped, whereas aerosols tend to spiral outward, therefore escaping and probably doing so faster than the fluid itself.

The dynamics of heavy particles in open flows is important in many fields. In astrophysics, it can provide a mechanism for the formation of planetesimals in the primordial solar nebula [6]. In geophysics, it has direct consequences for the transport and activity of pollutants and cloud droplets in the atmosphere [7]. It can also be useful for particle separation in industrial applications.

In this Letter, we show that the premise that aerosols in vortices tend to move outward does not necessarily imply that these particles will always escape faster in open flows. More remarkably, we show that aerosols much heavier than the advecting fluid can be *permanently trapped* in open chaotic advection. The mechanism affording the trapping of aerosols is associated with the occurrence of two or more vortices in a bounded region of the flow. In escaping from a vortex, the aerosols may enter the domain of another vortex, which in its turn may drive the particles back to the first vortex. This can lead to the formation of bounded stable orbits that give rise to attractors. We illustrate this phenomenon for two widely studied open flows: the *blinking vortex system*, which has static vortices, and the *leapfrogging vortex system*, which has moving vortices. These systems do not include any physical obstacle or boundary layer effect [8] that could mask the purely dynamical phenomenon we are interested in. The trapping of aerosols in open flows sharply contrasts with the behavior of the fluid particles, which escape and go to infinity with probability 1.

We start with the equation of motion for a small heavy spherical particle in a fluid flow. In dimensionless form, it reads [9]

$$\ddot{\mathbf{r}} = A(\mathbf{u} - \dot{\mathbf{r}} - W\mathbf{n}), \tag{1}$$

where $\mathbf{r}$ is the position vector of the particle, $\mathbf{u} = \mathbf{u}(\mathbf{r}(t), t)$ is the fluid velocity field evaluated at the particle's position, and $\mathbf{n}$ is a unit vector pointing upward in the vertical direction. The two parameters governing the dynamics are the inertia parameter A and the gravitational parameter W. They can be written in terms of the characteristic length L and velocity U of the flow, radius a of the particle, kinematic viscosity ν of the fluid, gravitational acceleration g, and densities ρ_p and ρ_f of particle and fluid, respectively. The defining equations for these parameters are $W = (2a^2\rho_p g)/(9\nu U\rho_f)$ and $A = R/St$, where $R = \rho_f/\rho_p \ll 1$ and $St = (2a^2U)/(9\nu L)$ is the Stokes number of the particle. In the case of a water droplet in air flow, for example, one has $\rho_f/\rho_p \sim 10^{-3}$.

We first consider the blinking vortex-source system [10]. This 2-dimensional system is periodic in time and consists of two alternately point sources in a plane. It models the alternate injection of rotating fluid in a large shallow basin. The blinking vortex-source system is described by the stream function

$$\Psi = -(K\ln r' + Q\phi')\Theta(\tau) - (K\ln r'' + Q\phi'')\Theta(-\tau), \tag{2}$$

where Θ stands for the Heaviside step function,

$\tau = 0.5T - (t \bmod T)$, and T is the period of the flow. Here, r' and ϕ' are polar coordinates centered at $(x, y) = (-1, 0)$, while r'' and ϕ'' are polar coordinates centered at $(1, 0)$. The parameters Q and K are the strengths of the source and vortex, respectively. The parameter Q is negative (in fact, positive values of Q define a vortex-sink system). Positive and negative values of K correspond, respectively, to counterclockwise and clockwise vortex motion. The sources are located at positions $(\pm 1, 0)$. For each half-period, the flow remains steady with only one of the sources open. In the time interval $0 < t \bmod T < 0.5T$, the open source is the one at $(-1, 0)$, whereas in the time interval $0.5T < t \bmod T < T$, the open source is the one at $(1, 0)$. The velocity field of the fluid flow is

$$\mathbf{u} = (u_x, u_y), \qquad u_x = \partial\Psi/\partial y, \qquad u_y = -\partial\Psi/\partial x. \tag{3}$$

The parameters Q, K, and T in Eq. (2) can be chosen to yield either a nonhyperbolic or a hyperbolic dynamics for the fluid particles (*passive advection*). For instance, for $Q = -20$, $K = -400$, and $T = 0.1$, the invariant set is nonhyperbolic as it consists of a chaotic saddle plus (at least) one Kolmogorov-Arnold-Moser (KAM) island. For $Q = -10$, $K = -160$, and $T = 0.1$, on the other hand, apparently there are no islands. Numerical calculations confirm that the survival probability of fluid particles in the neighborhood of the chaotic saddle decays exponentially fast, which is a signature of hyperbolic dynamics.

We now investigate the dynamics of aerosols governed by Eq. (1) in the flow given by Eqs. (2) and (3), both in the cases where the passive advection is hyperbolic and nonhyperbolic, and both in the absence and presence of gravity. As shown in Fig. 1, the trapping of aerosols in attractors can occur in all these cases. The figure shows, for different parameters, the projection into the physical space of the attractor at time instants $t \bmod T = 0$. The corresponding basins of attraction for initial velocities equal to the local velocities of the fluid are also shown. We note that the dynamics of the aerosols takes place in a 4-dimensional phase space, corresponding to the variables (x, y, v_x, and v_y) and is dissipative due to the drag term, whereas the dynamics of the fluid particles is 2 dimensional, since their velocity is a function of their position, and is conservative because the flow is incompressible. Despite the fact that, from the dynamical systems viewpoint, dissipation may give rise to attractors, we stress that we deal with *open* flows and that in this case the presence of dissipation *does not* imply the occurrence of attractors in a *bounded region*. In open systems, attractors may be formed at *infinity* in the physical space [5]. The trapping of aerosols is counterintuitive also in view of the fact that these particles move outward in vortices. Notwithstanding, Fig. 1 shows that this phenomenon is possible in a broad range of conditions. Figure 1(a) shows the occurrence of attractors for the dynamics of the aerosols when the underlying passive advection is nonhyperbolic. For small W and large A, the

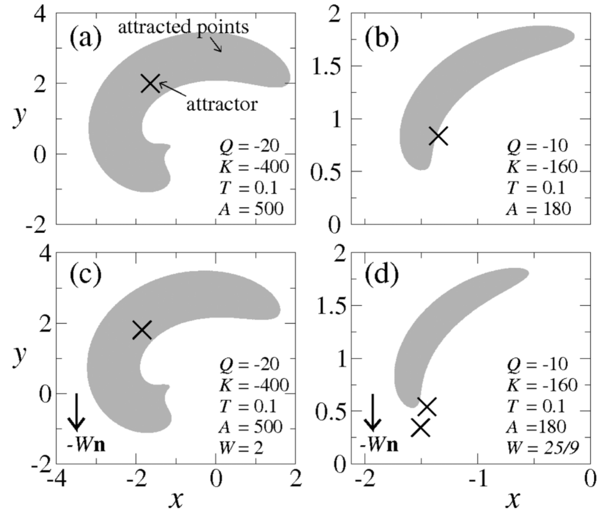

FIG. 1. Projection into the physical space of the stroboscopic section $t \bmod T = 0$ for the aerosol dynamics in the flow of Eq. (2). The black $\times$ symbols indicate the attractors and the gray areas the corresponding basins of attraction for initial velocities equal to the local velocities of the fluid at $t = 0$. (a) Nonhyperbolic and (b) hyperbolic passive advection in the absence of gravity; (c) nonhyperbolic and (d) hyperbolic passive advection in the presence of gravity. The attractors in (a)–(c) are period-one orbits, whereas the attractor in (d) is a period-two orbit. Note that the attractors are not necessarily inside the gray areas because these areas correspond to *subsets* of the basins of attraction defined by specific initial velocities. The gravity vector points in the negative direction of the y axis.

dynamics of the aerosols can be understood as a perturbation of the dynamics of the fluid particles [11]. As shown below, in this regime attractors can be formed in the KAM islands of the passive advection. In the case of Fig. 1(a), we are not in the limit of weak perturbation and the basin of attraction is actually larger than the KAM island itself. The appearance of attractors when the aerosols are advected by a *hyperbolic* passive dynamics is less expected, since hyperbolic systems are structurally stable. Nevertheless, the occurrence of attractors is possible also in this case, as shown in Fig. 1(b), and the reason again is that we are far from the weak perturbation limit. Attractors also occur when the gravitational effects are important, i.e., when W is of order of 1 or larger. As shown in Figs. 1(c) and 1(d), this is possible for both nonhyperbolic and hyperbolic passive advection. We consider that the gravitational field points along the y direction.

It is worth noting the rich variety of possibilities for the motion of aerosols under gravity, which includes both the trapping in smooth *open* flows described here, the suspension in random *closed* flows discussed in [12], and the increased average settling velocity when the aerosols are in an infinite, periodic, cellular fluid flow [13]. Note that the mechanism for suspension presented in [12] is based on the change of sign of the curvature of the streamlines while our mechanism is based on the vortex-to-vortex advection of the aerosols. In particular, the curvature of the streamlines of the blinking vortex-source system is one-signed and does not satisfy the conditions considered in [12].

The stroboscopic sections shown in Fig. 1 correspond to attractors that are simple periodic orbits. The full physical space projection of one such attractor is shown in Fig. 2(a). But strange attractors can also occur, as shown in Fig. 2(b). They are formed when either A or W is increased [see Figs. 2(c) and 2(d)]. The bifurcation diagrams are dominated by the period-doubling route.

The trapping of aerosols in open flows displaying chaotic advection is a general phenomenon. The dynamics defined by Eq. (1) is dissipative. In open flows, dissipation is not a sufficient condition for the occurrence of bounded attractors. However, this condition becomes sufficient in periodic flows if a set of initial conditions with positive volume is advected back to itself after one time period. In the case of bubbles, this condition is frequently satisfied because bubbles tend to remain inside closed orbits of the fluid particles generated by vortices [4,5]. This mechanism cannot explain the existence of attractors in the case of aerosols because, for heavy particles, rather the opposite happens due to the centrifugal force. However, when *multiple* vortices are present in the flow and remain confined to a bounded region, we show that a *different* mechanism can give rise to attractors in which the aerosols are trapped. The mechanism of trapping is in this case based on successive "escape attempts" from distinct vortices. As shown in Fig. 3, a possible outcome of the motion of aerosols outward successive vortices is the formation of bounded orbits. Trapping occurs if this happens for a set of orbits with positive volume, as shown for the blinking vortex system.

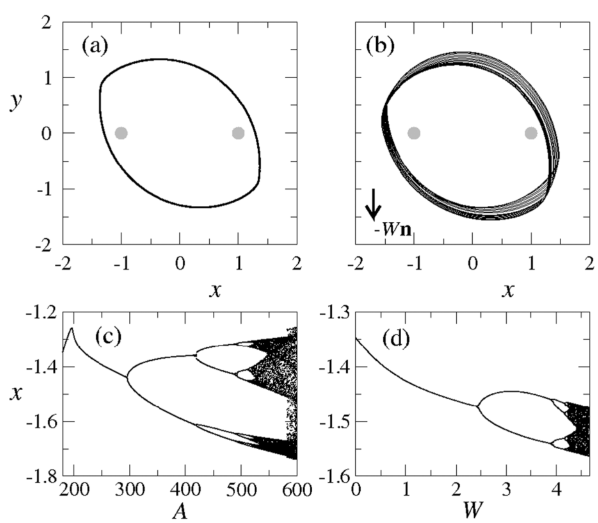

FIG. 2. (a) Periodic attractor corresponding to $W = 0$ and (b) strange attractor corresponding to $W = 40/9$. The gray dots represent the point sources. (c)–(d) Bifurcation diagrams showing the x coordinates of the attractor at time $t \bmod T = 0$ as a function of parameter A in the absence of gravity (c) and as a function of W when $A = 180$ (d). The unspecified parameters are the same as in Fig. 1(b).

To demonstrate the generality of our results, we now consider a system with moving vortices: the leapfrogging vortex system [14], which is a 2-dimensional flow consisting of two vortex pairs of equal strengths. As a consequence of mutual influence [15], these vortex pairs move along the direction of a symmetry axis that separates them. Denoting the positions of the vortices by $(x_1, \pm y_1)$ and $(x_2, \pm y_2)$ we take $x_1 = x_2 = 0$, $y_1 = 0.5$, and $y_2 = 1.5$ as the vortices coordinates at $t = 0$. The Hamiltonian $H(x_0, x_r, 2y_0, \frac{y_r}{2}) = 0.5 \ln\frac{[x_r^2+(2y_0)^2][(2y_0)^2-4(y_r/2)^2]}{[x_r^2+4(y_r/2)^2]}$ describes the periodic motion of the vortices, where $x_0 = (x_1 + x_2)/2$, $y_0 = (y_1 + y_2)/2$, $x_r = (x_2 - x_1)$, and $y_r = (y_2 - y_1)$. The stream function in a reference frame whose origin is the point $(x_0(t), 0)$ reads $\Psi(x, y, t) = \ln[(r_3 r_4)/(r_1 r_2)] - \dot{x}_0(t) y$, where $r_{1(2)}^2 = [x - x_{1(2)}(t)]^2 + [y - y_{1(2)}(t)]^2$ and $r_{3(4)}^2 = [x - x_{2(1)}(t)]^2 + [y + y_{2(1)}(t)]^2$. In this reference frame, the fluid particles come from $x = \infty$, are scattered in the region close to the origin, where the vortices are confined, and finally move toward the negative direction of the x axis. We have investigated the dynamics of aerosols in this flow and we found trapping for a broad range of the parameter A. Figure 4 illustrates the trapping of aerosols in this flow for $A = 50$ and $W = 0$.

In the general case of nonhyperbolic passive advection, we can demonstrate the formation of attractors explicitly for $A \gg 1$ and $W \ll 1$ using a first-order approximation [11] of the dynamics given by $\dot{\mathbf{r}} = \mathbf{u} - W\mathbf{n} - \frac{1}{A}[\frac{\partial \mathbf{u}}{\partial t} + (\mathbf{u} \cdot \nabla)\mathbf{u} - (W\mathbf{n} \cdot \nabla)\mathbf{u}]$. If $W \ll 1$ and the magnitude of the term inside the brackets is much smaller than A, the

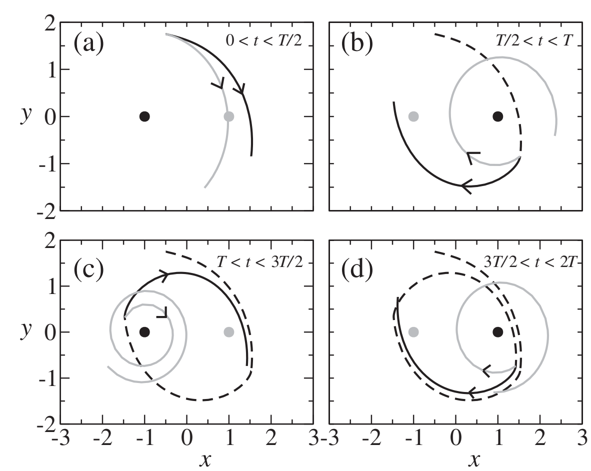

FIG. 3. Trajectories of an aerosol (black curve) and a fluid particle (gray curve) of the same initial position. In (a), the aerosol and the fluid particle also have the same initial velocity, whereas in (b)–(d) the aerosol simply continues the trajectory initiated in (a). The point source that is open during each time interval is shown as a black dot (the gray dot corresponds to the other one). The dashed lines represent the trajectory of the aerosol before the time interval indicated in the figure. After 2 periods of the fluid flow, the aerosol is already very close to a periodic attractor [cf. Fig. 2(a)]. The parameters are the same as in Fig. 1(b).

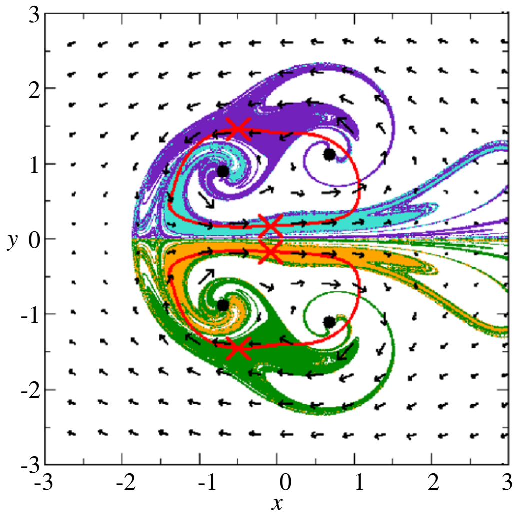

FIG. 4 (color online). Trapping of aerosols in the leapfrogging vortex flow: physical space projection of the 4 attractors [$\times$ (red) symbols] and corresponding basins of attraction (colored regions) for initial velocities equal to the fluid velocity at $t \bmod T = 0.8$, where T is the period of the flow. Also shown are the velocity field of the fluid (black arrows) and the positions of the vortices (black dots) at the same instant. The closed (red) curves indicate the orbits described by the attractors. See [16] for the animation.

dynamics corresponds to a small perturbation of the passive advection in a 2-dimensional effective phase space. If the divergence $\nabla \cdot \dot{\mathbf{r}}$ of the velocity field is negative, as in the blinking vortex-source system [17], KAM islands of the passive advection are expected to be transformed into basins of attraction. The formation of attractors in KAM islands has been observed in the advection of bubbles [5] and in the study of Hamiltonian systems [18]. However, in a very neat contrast with the mechanism previously considered in the study of bubbles, in the case of aerosols the KAM islands that give rise to attractors describe the dynamics of particles that *necessarily visit more than one vortex*. From the relation $\nabla \cdot \dot{\mathbf{r}} = (\omega^2 - s^2)/(2A)$ [11], we can see that in these islands the strain s must dominate over the vorticity ω. We emphasize, however, that the phenomenon of trapping of aerosols is far more general since it also occurs in nonperturbative regimes (small A and large W) and in the absence of KAM islands, as shown in Figs. 1–4.

In conclusion, we have shown the occurrence of trapping of heavy particles in open flows. This phenomenon does not depend on the nonhyperbolicity of the passive advection and is possible even when the gravitational effect is large. An experiment to demonstrate trapping in the leapfrogging vortex system could be done with air as the working fluid [19]. In this case, the condition $\rho_f/\rho_p \ll 1$ is fulfilled for virtually all solid and liquid particles. The trapping mechanism reported here provides a mechanism for the concentration of heavy particles in specific regions of the physical space. This may play a role in planetesimal formation in primordial nebula with rapidly rotating anticyclonic vortices, where the centrifugal force prevails over the Coriolis force. It may also be useful for particle-fluid and particle-particle (different size classes) separation in industrial applications.

We thank Ernesto Nicola, Edward Ott, Oreste Piro, Antonello Provenzale, and Tamás Tél for stimulating discussions.

[1] C. Jung *et al.*, Chaos **3**, 555 (1993).
[2] H. Kantz and P. Grassberger, Physica (Amsterdam) **17D**, 75 (1985); T. Tél, in *Directions in Chaos*, edited by Hao Bai-Lin (World Scientific, Singapore, 1990), Vol. 3, pp. 149–221.
[3] J. C. Sommerer and E. Ott, Science **259**, 335 (1993); L. Yu *et al.*, Physica (Amsterdam) **110D**, 1 (1997); L. Yu *et al.*, *Nonlinear Structure in Physical Systems* (Springer-Verlag, New York, 1990), pp. 223–231; A. Babiano *et al.*, *Coherent Structures in Complex Systems* (Springer-Verlag, Berlin, 2001), pp. 114–124.
[4] I. J. Benczik *et al.*, Phys. Rev. Lett. **89**, 164501 (2002); Phys. Rev. E **67**, 036303 (2003).
[5] A. E. Motter *et al.*, Phys. Rev. E **68**, 056307 (2003).
[6] P. Barge and J. Sommeria, Astron. Astrophys. **295**, L1 (1995); P. Tanga *et al.*, Icarus **121**, 158 (1996).
[7] J. H. Seinfeld, *Atmospheric Chemistry and Physics* (Wiley, New York, 1998); T. Tél *et al.*, Chaos **14**, 72 (2004); T. Tél *et al.*, Phys. Rep. **413**, 91 (2005).
[8] C. Marchioli and A. Soldati, J. Fluid Mech. **468**, 283 (2002).
[9] M. R. Maxey and J. J. Riley, Phys. Fluids **26**, 883 (1983); T. R. Auton *et al.*, J. Fluid Mech. **197**, 241 (1988); E. E. Michaelides, J. Fluids Eng. **119**, 233 (1997).
[10] H. Aref *et al.*, Physica (Amsterdam) **37D**, 423 (1989); G. Károlyi and T. Tél, Phys. Rep. **290**, 125 (1997).
[11] M. R. Maxey, J. Fluid Mech. **174**, 441 (1987).
[12] C. Pasquero *et al.*, Phys. Rev. Lett. **91**, 054502 (2003).
[13] M. R. Maxey and S. Corrsin, J. Atmos. Sci. **43**, 1112 (1986).
[14] A. Pentek *et al.*, J. Phys. A **28**, 2191 (1995).
[15] H. Aref, Annu. Rev. Fluid Mech. **15**, 345 (1983); A. Provenzale, Annu. Rev. Fluid Mech. **31**, 55 (1999).
[16] See EPAPS Document No. E-PRLTAO-99-080750 for the animation. For more information on EPAPS, see http://www.aip.org/pubservs/epaps.html.
[17] For the blinking vortex-source system, we find $\nabla \cdot \dot{\mathbf{r}} = -\frac{2(K^2+Q^2)}{A}[\frac{1}{r^4}\Theta(\tau) + \frac{1}{r'^4}\Theta(-\tau)] < 0$.
[18] M. A. Lieberman and K. Y. Tsang, Phys. Rev. Lett. **55**, 908 (1985); T. Pohl *et al.*, Phys. Rev. E **65**, 046228 (2002); A. E. Motter and Y.-C. Lai, Phys. Rev. E **65**, 015205 (2001).
[19] H. Yamada and T. Matsui, Phys. Fluids **21**, 292 (1978).